ICFO Challenge: Quantum Simulation with quantum computers

A. Azzam, H. Briongos, T. Krasimirov, J. Nogué, T. Parella, J. Romero

April 2, 2023

1 Spins in the ground state: The XXZ Heisenberg model

In this first section, we studied the XXZ Heisenberg model, represented by the Hamiltonian from Eq.(1).

$$H_{XXZ} = -\frac{1}{4}\sum_{i=1}^{N} \sigma_i^x \sigma_{i+1}^x + \sigma_i^y \sigma_{i+1}^y + \Delta\, \sigma_i^z \sigma_{i+1}^z \quad (1)$$

with Δ being a parameter that rules the behaviour of the system i.e. for $\Delta < -1$ the system is antiferromagnetic, for $\Delta \in [-1, 1]$ the system is paramagnetic and for $\Delta > 1$ the system is ferromagnetic. Moreover, it must be stated that we have specifically studied this model for 12 spins.

1.1 Ground state energy of the XXZ model

In this first section, we calculated the ground state energy of the XXZ Heisenberg model for $\Delta = 4, -2$. For $\Delta = 4$, we are in the ferromagnetic phase. Therefore, we proposed a initial state where all qubits are in the 0 state as we already know that in the ferromagnetic phase the ground state will have all spins pointing towards the same direction (in this case, the ground state is degenerate so it can have either all the spins up or all the spins down). Therefore, we encode the trivial state, $|0...0\rangle$ ($N = 12$) into a quantum circuit and calculate the expected value of the Heisenberg hamiltonian with the qiskit funciont *expectation_value($\hat{H}_{XXZ}$)*. Taking atomic units, we obtain the $\epsilon_{GS} = 12.0$, which agrees with the theoretical value for the ferromagnetic regime, explained in Eq.(2)

$$\epsilon_{GS} = -N\frac{\Delta}{4} \quad (2)$$

Regarding $\Delta = -2$, we found the ground state using the variational quantum eigensolver and we compared it with the result obtained by exact diagonalization. We performed the exact diagonalization following the two approaches:

1. By explicitly constructing the sparse matrix (to save memory) of the Hamiltonian and diagonalizing it with SCIPY.SPARSE.LINALG.EIGSH.
2. By using the exact diagonalization *NumPyMinimumEigensolver* embedded in qiskit QISKIT.ALGORITHMS. We tried different mappings but we could only diagonalize it using *LogaritmicMapper*.

For both approaches we obtained that the energy of the ground state is $\epsilon_{GS}(teo) \approx -7.46$.

1.1.1 VQE implementation

In this section we used a VQE implementation to calculate the ϵ_{GS} for $\Delta = -2$. We used a 3 layers of *TwoLocal* ansatz with rotations $R_x R_z R_x$ and circular conditions (to preserve boundary conditions) and the SPAS optimizer. We obtained that the energy of the groundstate is $\epsilon_{GS} \approx -3.95$, a result that is not close to the theoretical value, $\epsilon_{GS}(teo) \approx -7.46$. We believe that this result is due to a poor choice of the ansatz, in the following section we will try different circuit ansatz combined with various optimizers to obtain the best performance of the VQE.

1.2 Ansatz expressibility

In this section, we studied the effect of different ansatzs and optimizers in the VQE, still for $\Delta = -2$. We used 3-layers ansatzs, made of single qubit gates and two qubit gates with interactions between either (i) all qubit pairs (FIG.8) or (ii) only neighboring qubits (FIG.9). Moreover, we used 3 different optimizers; (i) Simultaneous Perturbation Stochastic Approximation-SPSA; (ii) Constrained Optimization by Linear Approximation-COBYLA and (iii) Sequential Least Squares Programming-SLSQP. To evaluate the performance of a pair of ansatz-optimizer, we tracked how many steps the optimizer took to converge (in our case, we plotted all the results and stopped the iterations when we saw that the algoritm stabilised). The results of this exploration are summarized in FIG.1. It's easy to see that SLSQP optimizer is not improving with neither of the anstatz, and is automatically discarded. For the other two optimiz-

ers, the most accurately one is SPAS but it takes much longer to finish the optimizing loop, while the COBYLA stops much earlier, with the drawback that it doesn't provide as good results as the first one. Also, for both cases the circular with just neighbours entanglement ansatz is way better than the fully connected one. This comes to an agreement with the fact that the Heisenberg hamiltonian only has interactions with nearest neighbours so it makes physical sense that an ansatz with qubit pairs interactions obtains better results.

Therefore, we will consider the COBYLA circular optimizer for section 2, as we trump the faster convergence of the algorithm than its precision when it comes to complex simulations. On the other hand, we will use the SPSA circular optimizer to calculate the phase diagrams, as it is slower but more precise, and we need precision to tackle phase transitions.

1.3 Phase diagram

In this third and last section of the first problem of the challenge, we computed the magnetization, staggered magnetization and the nearest neighbour correlator (eq 3-5 respectively) of the ground state of our system as a function of the parameter Δ.

$$M = \frac{1}{2N}\sum_{i}^{N}\langle\hat{\sigma_i^z}\rangle \tag{3}$$

$$M_{st} = \frac{1}{2N}\sum_{i}^{N}(-1)^i\langle\hat{\sigma_i^z}\rangle \tag{4}$$

$$C = \frac{1}{4N}\sum_{i}^{N}\langle\sigma_i^z\sigma_{i+1}^z\rangle \tag{5}$$

We have started by computing the ground state for a given delta by means of the variational quantum eigensolver already used in the previous sections for the SPSA circular optimizer. Once we found the ground state, we calculate the respective expectation values needed to compute the aforementioned physical magnitudes. In other words, for each Δ, we obtain an optimized set of circuit parameters $\{\tilde{\theta}\}$ through VQE. We used two different approaches to calculate the expectation value of the different operators with $\{\tilde{\theta}\}$:

1. We re-created our initial target ansatz with the optimized parameters $\{\tilde{\theta}\}$ obtained from VQE. We calculated the state vector associated to this optimized quantum circuit and applied the previously used function *expectation_value($\hat{A}$)* to calculate the expectations values of the magnestisation, staggered magnetisation and NN correlator as a function of Δ (FIG.2).

2. Again taking the original ansatz with the optimized parameters $\{\tilde{\theta}\}$ obtained from VQE, we performed a set of measurements of the circuit with an Aer backend. Since the measurements are in the computational basis, we calculated the expected values of the magnestisation, staggered magnetisation and NN correlator with the statistics of the measurements (FIG.3).

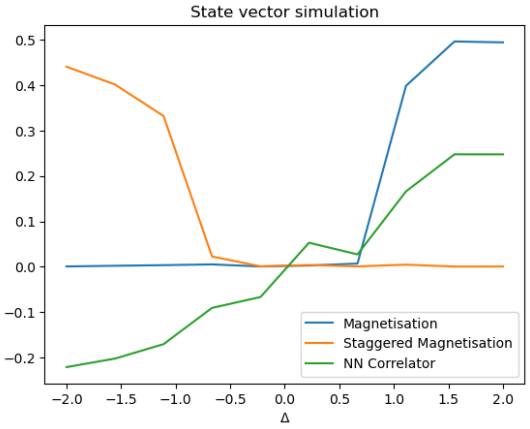

Figure 2: Expectation values as a function of Δ, calculated from the state vector of the optimized quantum circuit ansatz.

In the phase diagram we can clearly see the three expected phases. For $\Delta < -1$ the system behaves as ferromagnetic. We can see that the magnetization is 0, which means that half of the spins are pointing to each direction, and the correlation is negative and maximum ($C = -1/2 \times 1/2 = -0.25$) highlighting that between neighbours, spins are antiparallel.
For $\Delta \in [-1, 1]$ the system behaves as paramagnetic because both magnetization and staggered magnetisation are zero, meaning that spins are on average randomly up and down and the correlation is almost vanishing.

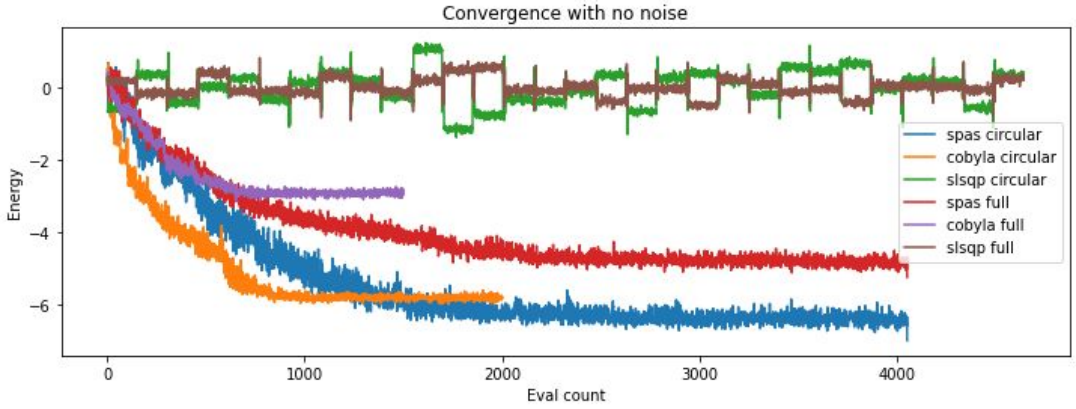

Figure 1: Convergence of the different combinations of ansatz-optimizer.

For $\Delta > 1$ the system is ferromagnetic, with all spins aligned in the same direction giving the maximum value of magnetization ($\langle M \rangle = 1/2$, since we have spin-1/2) and correlation $C \approx 0.25$.

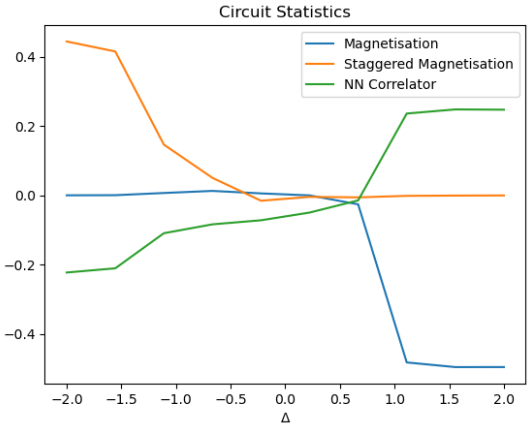

Figure 3: Expectation values as a function of Δ, calculated from the measurement of the optimized quantum circuit ansatz.

We also notice the difference between the two figures, FIG.2 and FIG.3, where the magnetization value for $\Delta > 1$ takes opposite sign. This difference appears due to the degeneracy of the ferromagnetic groundstate where all spins are aligned but both directions appear with the same probability. To obtain the results of FIG.2, we added an additional magnetic field pointing to the z axis term to the Heinsenberg hamiltonian to break the symmetry of the groundstate. Due to time constraints (as mentioned, the SPSA circular optimizer was precise but slow), the calculations regarding the circuit statistics were run without the degeneracy-breaking term, and statistical fluctuations made the ground state for big values of Δ to be opposite-aligned as the one found using the statevector strategy. An example to show that both options of groundstates appear for some instances of VQE minimizations is shown in figures 10 and 11, where for consecutive values of $\Delta > 1$, we obtained the states $|000...0\rangle$ and $|111...1\rangle$.

2 Fermions in excited states: Lithium Hydride

2.1 Molecular spectra

We performed a simulation of the LiH spectrum at a bond length of 2.0 Å, using a STO-3G minimal basis. The ground, first, and second excited states were simulated variationally, with an active space of 10 spin-orbitals. To facilitate the mapping between the second quantization Hamiltonian and the qubit Hamiltonian, we used parity mapping as the fermion-to-qubit mapping method. We implement the general results for different bond lengths in the following section.

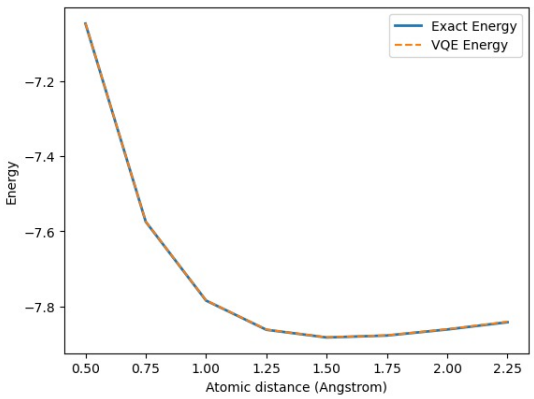

Figure 4: VQE and exact energies as a function of the bond length.

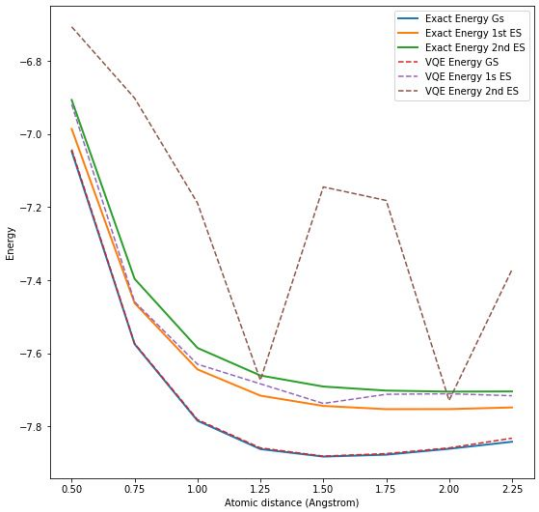

Figure 5: Theoretical and VQD energies for the ground and first two excited states.

2.2 Spectrum as function of bond length

We have conducted a comparative analysis of the ground state energy obtained through exact diagonalization and VQE as a function of bond distance FIG.4. For the VQE calculation, we utilized the UCCSD circuit ansatz and SLSQP optimizer. Additionally, we extended our spectral energy calculations to the first two excited states using the Variation Quantum Deflation (VQD) method with UCCSD circuit ansatz and COBYLA optimizer. The results of the exact diagonalization and VQE energies as a function of bond distance are shown in FIG5, while FIG6 displays the energy differences between exact and VQE for each computed state. We observed accurate VQE calculation for the ground state with an error of approximately 0.01 Hartree.

However, there was an increasing energy deviation for the excited states, with the first excited state exhibiting a maximum error of about 0.8 Hartrees and the second excited state being the least accurate. This deviation was attributed to the VQD orthogonalization constraints, which were sequentially applied during the algorithm, resulting in the errors of the first excited state being carried over to the second excited state, which was orthogonalized to the non-error-free first excited state.

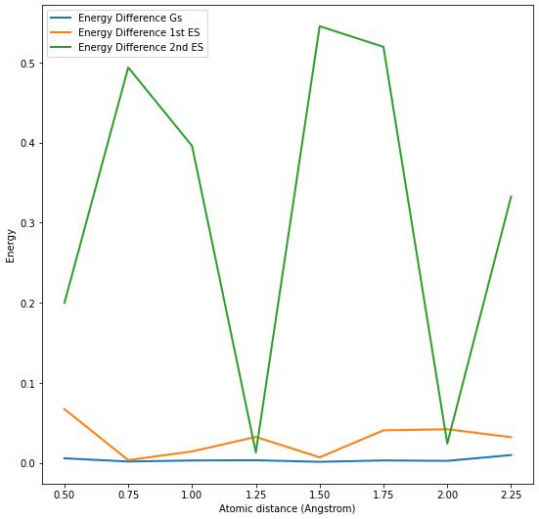

Figure 6: Absolute error between VQE and exact energies for the ground and first two excited states.

2.3 Imperfect devices

In this last section, we have proceeded to repeat the simulation but adding a 0.02 error rate to the 2-qubit controlled-X gates to simulate a noisy/imperfect device. UCCSD has been used as anzatz in first instance to simulate a noisy approach. The code has run during 323 minutes to

execute on an i7 intel core processor and the results were bad as expected. We obtained a value for the energy, with a bond distance of 1.56, of -5.63126, when the expected value was supposed to be -7.84154057. Moreover, for the first excited state we obtained a value of -5.14872 when we were expecting -7.74779504. These results were expected as the UCCSD circuit is very large so even a small error such as 2% would have large implications on the energy of the model.

UCCSD anzatz has been substituted due to the large amount of parameters on the system and the incapacity of convergence from the method. Instead, we have considered multilayers of parametrized global unitaries 'X'+'Z'+'X' gates and controlled-X gates. We have studied the trade-off between the complexity of the system and the amount of noise arising from controlled-X gates. Results of the spectral energy (both with VQD and exact) as function of layers is displayed in FIG7.We observe that with 1 layer, the number of variational parameters is already 24. Best performance is achieved with a single layer, proving how transcendental the implications of noise are.

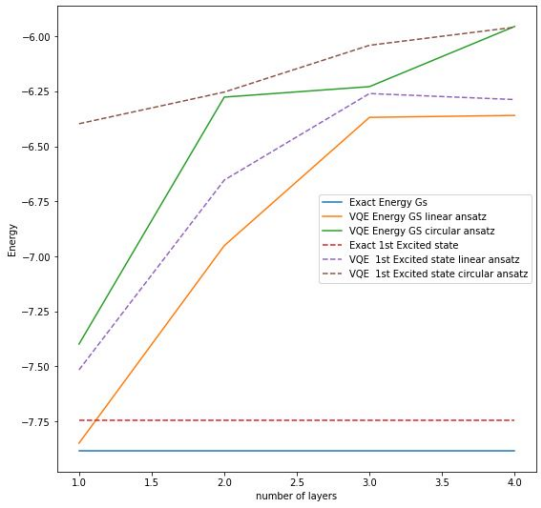

Figure 7: Energy as a function of the number of (XZX + CX) layers used to construct the ansatz.

3 Master the quantum simulation shenanigans

Similar to our previous experiences, when running the circuit on a real quantum computer, several factors can influence the accuracy of our energy measurement. On a real device the noise model extends beyond the controlled-Not gate, and covers all single and double qubit gates. Moreover, real devices suffer some errors when reading the value of a qubit or due to the connections between two physical qubits.

All these factors contribute to the resulting energy of the VQE simulation being far from the energy obtained by the exact diagonalization. The energy of the ground state that we obtained for the H_2 molecule using a simulated backend with noise model that maps the real device was -0.98902 whereas the real value of the ground state energy is -1.2942. Moreover, the energy of the first excited state that we obtained was -0.43102 while the value we were expecting was -0.84900.

While trying to run the VQE in the real quantum computer (ibm-jakarta) to find the H_2 molecule ground state, the job was stuck during 4 hours in what seemed an infinite loop judging by the logs of the job after hard-stopping it.

In order to reduce some sources of error from the gates, one could try to calibrate the basic quantum operators that physically rely on beam pulses causing the desired transformation. Given that these transformations are performed using light pulses, the point would be to directly sweep through the frequencies testing for which one the transformation gives the less-noisy result, this is, the closest one to the theoretical resulting quantum state. This approach would result into gates with more fidelity and more accurate measurements.

Due to the high complexity of UCCSD ansatz optimization in the noisy model, we have observed that simpler approaches such as a single layer XZX+CX approach performs best by leveraging shallow circuit depth. Further approaches could be taken in this layer direction by efficiently performing zero noise extrapolation by tracking noise dependancy on layer usage. However, due to the limited time of the hackathon, we leave this implementations to future work. On top of this, we remark that although having tried the transpilation

function implemented in qiskit, no error mitigation advantages have been experienced. We believe that superior error mitigation could be achieved by improving transpilation function quality.

Note:

WE tried to run the code on a real quantum computer, with measurement error mitigation turned on and reducing the depth of the circuit to see the performance of the computer. However the job ran for over 3 hours and got stuck in an internal infinite loop. We stopped eventually and started a new job without the error measurement error mitigation hopping that it would reduce the runtime however we were waiting in the queue and didn't have enough time to actually execute it.

A Additional figures

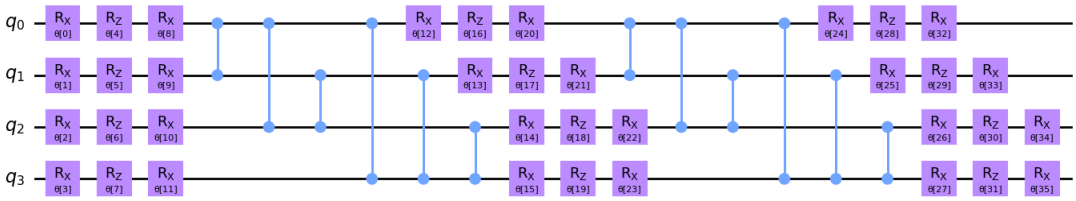

Figure 8: 2-layer with four qubits circuit ansatz, with connections between all qubit pairs

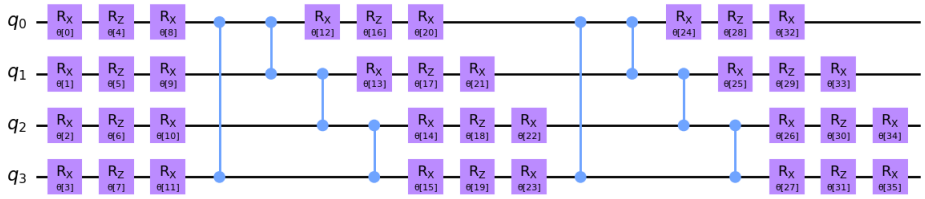

Figure 9: 2-layer with four qubit circuit ansatz, with connections only with nearest neighbours.

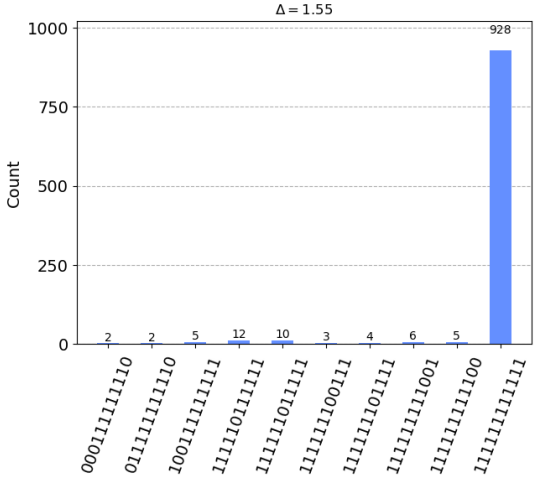

Figure 10: Instance of histogram for $\Delta = 1.55$

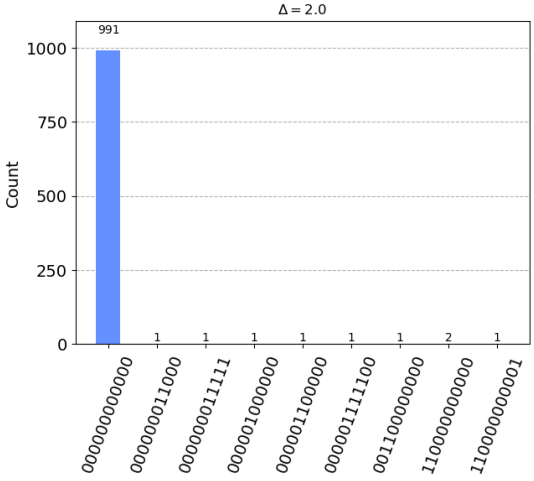

Figure 11: Instance of histogram for $\Delta = 2.0$